Title

High-Fat, High-Calorie Diet Promotes Early Pancreatic Neoplasia in the Conditional KrasG12D Mouse Model

Journal

Cancer Prevention Research, 6(10)

ISSN

1940-6207

Authors

Dawson, David W
Hertzer, Kathleen
Moro, Aune
et al.

Publication Date

2013-10-01

DOI

10.1158/1940-6207.capr-13-0065

Peer reviewed

Published in final edited form as:
Cancer Prev Res (Phila). 2013 October ; 6(10): . doi:10.1158/1940-6207.CAPR-13-0065.

High Fat, High Calorie Diet Promotes Early Pancreatic Neoplasia in the Conditional Kras^{G12D} Mouse Model

David W. Dawson[3,5], **Kathleen Hertzer**[1], **Aune Moro**[1], **Graham Donald**[1], **Hui-Hua Chang**[1], **Vay Liang Go**[2], **Steven J. Pandol**[2,6,7], **Aurelia Lugea**[2,6], **Anna S. Gukovskaya**[2,6], **Gang Li**[4,5], **Oscar J. Hines**[1,5], **Enrique Rozengurt**[2,5], and **Guido Eibl**[1,5]

[1]Department of Surgery, UCLA Center for Excellence in Pancreatic Diseases, David Geffen School of Medicine at UCLA

[2]Department of Medicine, UCLA Center for Excellence in Pancreatic Diseases, David Geffen School of Medicine at UCLA

[3]Department of Pathology and Laboratory Medicine, UCLA Center for Excellence in Pancreatic Diseases, David Geffen School of Medicine at UCLA

[4]Department of Biostatistics, School of Public Health at UCLA

[5]UCLA Jonsson Comprehensive Cancer Center

[6]Department of Medicine, Veterans Affairs Greater Los Angeles Health Care System

[7]Department of Internal Medicine, Cedars Sinai Medical Center

Abstract

There is epidemiologic evidence that obesity increases the risk of cancers. Several underlying mechanisms, including inflammation and insulin resistance, are proposed. However, the driving mechanisms in pancreatic cancer are poorly understood. The goal of the present study was to develop a model of diet-induced obesity and pancreatic cancer development in a state-of-the-art mouse model, which resembles important clinical features of human obesity, e.g. weight gain and metabolic disturbances.

Offspring of Pdx-1-Cre and LSL-KrasG12D mice were allocated to either a diet high in fats and calories (HFCD; ~4,535 kcal/kg; 40% of calories from fats) or control diet (CD; ~3,725 kcal/kg; 12% of calories from fats) for 3 months. Compared to control animals, mice fed the HFCD significantly gained more weight and developed hyperinsulinemia, hyperglycemia, hyperleptinemia, and elevated levels of IGF-1. The pancreas of HFCD-fed animals showed robust signs of inflammation with increased numbers of infiltrating inflammatory cells (macrophages and T-cells), elevated levels of several cytokines and chemokines, increased stromal fibrosis, and more advanced PanIN lesions.

Our results demonstrate that a diet high in fats and calories leads to obesity and metabolic disturbances similar to humans and accelerates early pancreatic neoplasia in the conditional KrasG12D mouse model. This model and findings will provide the basis for more robust studies attempting to unravel the mechanisms underlying the cancer-promoting properties of obesity as well as to evaluate dietary- and chemo-preventive strategies targeting obesity-associated pancreatic cancer development.

Corresponding Author: Guido Eibl, Department of Surgery, David Geffen School of Medicine, University of California at Los Angeles, 10833 LeConte Avenue, 72-236 CHS, Los Angeles, CA 90095. Phone: 310-825-5743; Fax: 310-825-8975; Geibl@mednet.ucla.edu.

Disclosures: The authors have nothing to disclose

Keywords

Obesity; inflammation; pancreatic intraepithelial neoplasia; tumor promotion; mouse model

Introduction

Pancreatic ductal adenocarcinomas (PaCa) is one of the most lethal human diseases, with overall 5-year survival rate of only 3–5% and a median survival period of 4–6 months. The incidence of this disease in the US has increased to more than 45,000 new cases in 2012 and is now the fourth leading cause of cancer mortality in both men and women (1). As the current therapies offer very limited survival benefits, novel therapeutic and preventive strategies are urgently needed to treat this aggressive disease.

It is generally accepted that PaCa arises through the progression of precursor lesions called PanINs (pancreatic intraepithelial neoplasias) (2,3). Importantly, early-stage PanIN lesions already contain genetic alterations, which are also found in PaCa (4). Essentially, all invasive PaCa contain an activating Kras mutation, which can also be detected in early PanINs (5). These observations led to the step-wise carcinogenesis paradigm, in which Kras mutations are characterized as early, initiating events. This notion is strongly supported by genetically engineered animal models, in which the expression of mutated Kras in PaCa progenitor cells during embryogenesis leads to the faithful recapitulation of PanIN development and step-wise progression (6). However, in this conditional Kras mouse the development of PaCa occurs late (after ~12 months) and only in few animals (~5–10%) (6). Mutated Kras seems to be necessary but not entirely sufficient for the development of invasive PaCa. The presence of another mutation, e.g. in the *Trp53* or *Ink4a/Arf* tumor suppressor genes, greatly accelerates PaCa development (7,8). In addition to its role in cancer initiation, oncogenic Kras is also required for the maintenance of primary and metastatic pancreatic cancer (9). Importantly, besides additional genetic alterations, changes in the pancreatic microenvironment, e.g. inflammation, also seem to promote PaCa development (10). Overall, the importance of Kras mutations in PaCa initiation is well accepted, while factors, either genetic or environmental, that promote tumor development are much less understood.

In addition to smoking, chronic pancreatitis and a family history of PaCa, epidemiological studies have linked obesity (and long-standing type 2 diabetes mellitus) with increased risk for developing PaCa and other clinically aggressive cancers (11–15). A recent analysis of a large, pooled set of studies included in the National Cancer Institute (NCI) Pancreatic Cancer Cohort Consortium (PanScan) has provided strong support for a positive association between obesity and increased risk of PaCa (16). There is mounting evidence that a high fat, high caloric diet, typical in Western societies, can lead to obesity and functions as a tumor promoting factor in PaCa (17–21). Several earlier studies indicated that high fat diets enhanced pancreatic carcinogenesis and tumor promotion but did not provide a satisfactory animal model for further mechanistic studies. For example, high fat diets enhanced pancreatic carcinogenesis in N-nitrosobis(2-oxopropyl)amine (BOP)-treated hamsters (17,22,23). Although BOP-treated hamsters develop dysplastic, PanIN-like lesions in the pancreas, this model is hampered by the fact that the chemical carcinogen BOP is capable of inducing various unknown mutations in the pancreas and extra-pancreatic tissues. A similar drawback exists in another study demonstrating that a high fat/high protein diet promoted chemical carcinogen-induced pancreatic cancer development in rats (20). In a murine tumor implantation model, a high fat diet induced obesity and stimulated pancreatic cancer growth (24). These studies did not use a genetic model and thus did not recapitulate the human disease. Recent genetically-engineered mouse models of pancreatic cancer support a causal

relationship between high dietary fat and pancreatic cancer but show disadvantages as a model system. A diet rich in omega-6 polyunsaturated fatty acids increased the frequency of pancreatic neoplasia but acinar cell-specific promoters were used (25). In another study, mice with a pancreas-specific activation of oncogenic Kras fed a high fat diet showed significant accelerated development and progression of PanINs (26). Further experiments showed that the tumor promoting effects of the high fat diet were mediated by a low-grade systemic inflammation, as PanIN development was attenuated on a TNF-α receptor-deficient background. However, in that study animals on the high fat diet did not gain more weight than control animals and remained insulin sensitive. The high fat diet led to pancreatic exocrine insufficiency (intestinal malabsorption with steatorrhea) with dramatic changes in energy metabolism, which collectively contributed to an improved glucose tolerance in these mice (26).

The goal of the present study was to develop a model of diet-induced obesity and pancreatic cancer development in a state-of-the-art mouse model, which resembles several important clinical features of human obesity, e.g. weight gain and metabolic disturbances. This model would be ideal to unravel underlying mechanism and to evaluate preventive strategies. The importance and feasibility of genetically-engineered mouse models for cancer prevention research has been highlighted recently (27–29). We used the conditional KrasG12D mouse model, which was developed by Tuveson and colleagues (6). This model is characterized by the progressive development of PanIN lesions over several months with a low penetration of invasive pancreatic cancer. We hypothesized that the slow development of pancreatic cancers in this model can be accelerated by dietary factors, acting as tumor promoters in KrasG12D-initiated pancreatic cells.

Materials and Methods

Conditional Kras^{G12D} mouse model

To study the effect of a high fat, high caloric diet on pancreatic cancer development, the conditional Kras^{G12D} model from Hingorani and colleagues was used (6). *LSL-KRAS*^{G12D} and *PDX-1-Cre* mice were maintained as heterozygous lines. After weaning, offspring of *LSL-KRAS*^{G12D} and *PDX-1-Cre* mice were fed either a high fat, high calorie diet (HFCD) or a control diet (see below) for 14 weeks. Individually-tagged mice had free access to diet and water. Food intake and body weight of each animal were measured twice weekly. After 14 weeks, animals were euthanized and the entire pancreas and other organs were harvested for further analyses. Animal studies were approved by the Chancellor's Animal Research Committee of the University of California, Los Angeles in accordance with the NIH Guide for the Care and Use of Laboratory Animals.

Experimental diets

The diets were obtained from Dyets, Inc., Pennsylvania (Table 1). A slightly modified AIN-76A purified rodent diet served as a control diet. Compared to the control diet our HFCD has increased caloric content (4,536 kcal/kg vs. 3,726 kcal/kg), which stems from an increase in corn oil-based fat content (1,800 kcal/kg vs. 450 kcal/kg). While ~12% of the total calories in the AIN-76A control diet come from fat, about 40% of total caloric intake in the HFCD stems from fat. The corn oil contains about 60% omega-6 polyunsaturated fatty acids (linoleic acid), saturated fatty acids (10.8% palmitic, 2.1% stearic), mono-unsaturated fatty acids (26.5% oleic), and small amounts of omega-3 polyunsaturated fatty acids (0.6% linolenic). Importantly, the amount of sucrose, salts, and vitamins are kept identical in both diets. To compensate for the increase in corn oil, we reduced the amount of cornstarch in the HFCD accordingly. The diets were handled under low light conditions, and stored at −20°C.

The diets were replaced twice weekly. The stability of the fatty acids in the diets was regularly monitored by the UCLA Nutritional Biomarker and Phytochemistry Core.

Genotyping analysis

Before randomization to the diets the presence of the *Kras*^{G12D} and *Cre* allele were determined by PCR analysis of genomic DNA, as described elsewhere, obtained from ear biopsies (30). Animals with both the *Kras*^{G12D} and *Cre* allele were designated as mutant (*KRAS*$^{+/G12D}$) and animals with neither the *Kras*^{G12D} nor the *Cre* allele were deemed wildtype (*KRAS*$^{+/+}$). At the end of the study at sacrifice the successful excision-recombination events were confirmed by PCR by the presence of a single LoxP site in the pancreas as described elsewhere (30).

Metabolic panel

Serum levels of insulin, insulin-like growth factor-1 (IGF-1), glucose, and leptin were measured using the MILLIPLEX MAP Mouse Endocrine Panel (Millipore, St. Charles, Missouri) according to the manufacturer's instructions. Briefly, serum samples were obtained and a dipeptidyl peptidase 4 (DPP IV) inhibitor was added to the samples. Standards, controls, and samples were added together with the prepared antibody-immobilized beads to a 96-well Microtiter Filter Plate and incubated on a plate shaker overnight at 4°C. After washing, biotinylated detection antibodies were added and incubated on a plate shaker for one hour at room temperature. Then, streptavidin-phycoerythrin conjugates were added and incubated for an additional 30 minutes. After thorough washing, the plate was read on a Bioplex 200 (Bio-Rad) with Bio-Plex Manager 5.0 software. According to the manufacturer, the assay sensitivity for insulin and all other analytes is 55.6 pM and 6.2 pM, respectively, with an intra- and inter-assay precision of 3.8–10.6% and 4.8–20.7%, respectively, a recovery in serum matrix for all analytes of about 100%, and no or negligible antibodies cross-reactivity. For measurements of cholesterol and tryglycerides, serum was separated by centrifugation at 5000 rpm for 10 minutes at room temperature. Serum samples were then stored at −80°C until used in serum chemistry assays. Serum chemistry was obtained by the UCLA Division of Laboratory Animal Medicine.

Inflammation score

Full histologic cross-sections of each pancreas were stained with hematoxylin and eosin for histopathologic examination by a gastrointestinal pathologist (D.D.) blinded to treatment conditions. Chronic pancreatitis was graded using a semi-quantitative scoring system, as previously described (31), with slight modification. Chronic pancreatitis was given an index score (0–12) reflecting the sum of scores for acinar loss, lobular inflammation, and fibrosis. Acinar loss was based on the percentage loss across the entire cross-section and graded as 0, absent; 1, 1–25%; 2, 26–50%; 3, 51–75%; and 4, >75%. Inflammation was based on the average number of lobular inflammatory cells per 40× high power field (HPF) (as counted in 10 non-overlapping HPFs) and graded as 0, absent; 1, 1–30 cells; 2, 31–50 cells; 3, 51–100 cells; and 4, >100 cells. Fibrosis was based on the cumulative area of stromal fibrosis across the entire pancreas and graded as 0, absent; 1, 1–5%; 2, 6–10%; 3, 11–20%; and 4, >20% fibrosis.

Evaluation of PanINs

Formalin-fixed, paraffin-embedded tissues were sectioned (4 μm) and stained with H&E. Six to eight sections (100 μm apart) of pancreatic tissues were histologically evaluated by a gastrointestinal pathologist blinded to the experimental groups. Murine PanIN lesions (mPanIN) were classified according to histopathologic criteria as recommended elsewhere (32) To quantify the progression of PanIN lesions, the total number of ductal lesions and

their grade were determined. Only the highest grade lesion per pancreatic lobule was evaluated. About 100 pancreatic ducts of the entire fixed specimen (head, body, and tail of the pancreas) were analyzed for each animal. The relative proportion of each mPanIN lesion to the overall number of analyzed ducts was recorded for each animal.

Fibronectin and α-SMA staining in mouse pancreas

Fibronectin and α-SMA expression, as indicative of stellate cell activation, was evaluated in formalin-fixed mouse pancreatic tissue sections by conventional immunofluorescence techniques. Sections were stained with primary antibodies against fibronectin (F3648) or α-SMA (A2547; both from Sigma-Aldrich) and Alexa Flour conjugated secondary antibodies (Life Technologies, Grand Island, NY). Nuclei were counterstained with DAPI. Stained sections were examined using a Nikon Eclipse-E600 fluorescence microscope equipped with a monochrome camera (CoolSnap, Roper Scientific, Germany) and the MetaMorph imaging system (Universal Imaging Corporation, PA). Digitized pictures were captured from multiple random, non-overlapping sections under a high-power field (× 400-magnification, 5–10 random fields per sample) with all exposures manually set at equal times and intensity values. The extent of fibronectin and α-SMA staining in stroma areas was determined by morphometric analysis using the MetaMorph imaging system (Universal Imaging Corporation, PA).

Immunohistochemistry

Paraffin-embedded sections were cut at 4 μm thickness and paraffin removed with xylene and rehydrated through graded ethanol. Endogenous peroxidase activity was blocked with 3% hydrogen peroxide in methanol for 10 min. Heat-induced antigen retrieval (HIER) or proteolytic induced epitope retrieval (PIER) were used. Sections were stained with antibodies against CD45R/B220 (BD Bioscience, cat.# 550286, 1:50 dilution for 2 hours), α-CD3 (DakoCytomation, Cat.# A0452, 1:100 dilution for 1 hour), or F4/80 (Serotec, cat # MCA497b, 1:50 dilution overnight) and appropriate secondary antibodies. Protein-antibody complexes were visualized with the Betazoid DAB Chromogen Kit (Biocare Mecdical, cat. #BDB2004L).

Cytokine Multiplex Array

Approximately 100 mg of isolated and previously snap-frozen mouse pancreas was defrosted on ice and homogenized with a mechanical homogenizer in 400–500 μl of 1X PBS pH 7.2, 1 mM PMSF (Sigma-Aldrich, St. Louis, MO) with protease inhibitors (Complete Protease Inhibitor Cocktail Tablet, Roche, Mannheim, Germany) and subsequently sonicated. Lysates were then centrifuged at 4°C for 15 minutes at 14,000 rpm and the supernatant was separated from the pellet. Protein concentrations of each lysate were then determined by BCA protein assay (Thermo Scientific, Rockford, IL) with BSA as a standard. Lysates were then immediately used for multiplex assays. Lysates were diluted to 5000 or 500 μg/ml total protein concentration and applied to a mouse cytokine magnetic bead panel (EMD Millipore, Darmstadt, Germany). Duplicates of each concentration were incubated overnight on a rotary orbital shaker at 4°C. Plates were then processed as recommended by the manufacturer and samples were run using a Bio-Plex 200 HTF Analyzer Luminex system (Bio-Rad, Hercules, CA). Data was obtained with Bio-Plex Manager 6.1 software (Bio-Rad, Hercules, CA) and further analyzed with Microsoft Excel.

Statistical analysis

Data are presented as mean ± SD. Differences in the mean of two samples were analyzed by an unpaired t test. Comparisons of more than two groups were made by a one-way ANOVA

with post hoc Holm-Sidak analysis for pairwise comparisons and comparisons versus control. An α-value of 0.05 was used to determine significant differences.

Results

A diet high in fats and calories leads to obesity and metabolic disturbances in mice

After weaning, offspring of *LSL-KRAS*^{G12D} × *PDX-1-Cre* intercrosses (pure C57BL/6 background) were randomly assigned to an AIN-76A-based control diet or a diet rich in fats and calories (HFCD; n=50 each). Compared to the control diet our HFCD has increased caloric content (4,536 kcal/kg vs. 3,726 kcal/kg), which stems from an increase in corn oil-based fat content (1,800 kcal/kg vs. 450 kcal/kg). While ~12% of the total calories in the AIN-76A control diet come from fat, about 40% of total caloric intake in the HFCD stems from fat (table 1). After 14 weeks, mice fed the control diet gained 7.2±2.8g, while mice fed the HFCD increased their body weight by 15.9±3.2g (Fig. 1A, B; $p<0.05$). We did not observe any difference in food consumption between both groups. In addition, there was no difference in weight gain between female and male mice (Fig. 1C). The development of obesity in HFCD-fed mice was visualized by micro-CT, which showed a marked increase in subcutaneous and visceral fat (Fig. 1D).

To assess whether the increase in body weight was associated with metabolic disturbances, we measured serum levels of insulin, glucose, IGF-1, and leptin. We found that mice fed the HFCD in comparison to control diet-fed animals displayed higher levels of insulin (501±311pM vs. 223±123pM; $p=0.047$), glucose (305±58mg/dl vs. 235±71mg/dl; $p=0.034$), IGF-1 (8.4±6.5ng/dl vs. 3.1±1.2ng/dl; $p=0.048$), and leptin (1375±276pM vs. 515±243pM; $p<0.01$) (Fig. 2). There was no significant difference in serum triglycerides and cholesterol levels between HFCD- and CD-fed mice (Fig. 2). A separate analysis after genotyping at sacrifice revealed no significant difference in weight gain and metabolic parameters between wildtype (*KRAS*$^{+/+}$) and mutant mice (*KRAS*$^{+/G12D}$).

A diet high in fats and calories leads to an inflammatory pancreatic microenvironment in mice

To assess the impact of the HFCD on initiation and maintenance of an inflammatory microenvironment in the pancreas, we histologically evaluated pancreatic tissue sections of mice fed the control and HFCD for the presence of intact acini (and conversely acinar cell loss), number of inflammatory cells, and percentage of stromal fibrosis. As described earlier, each parameter was quantitatively assessed and assigned a score (31). The sum of all individual scores constitutes the pancreatitis index (0– 12). Histological analysis revealed that wildtype mice fed the control diet had essentially no acinar cell loss, negligible inflammatory cell infiltration, and no stromal fibrosis resulting in a pancreatitis index of 0.4±0.5. Wild type mice fed the HFCD, however, showed minor acinar cell loss, a moderate infiltration of inflammatory cells, and weak stromal fibrosis, resulting in a pancreatitis index of 4.4±1.7 (Fig. 3A, B). Similar to wildtype mice fed the control diet, control diet-fed mutant mice (*KRAS*$^{+/G12D}$) had minimal loss of acinar cells, negligible inflammatory cell infiltration, and weak stromal fibrosis (pancreatic score of 1.3±0.6). Mutant mice fed the HFCD showed more robust signs of pancreatic inflammation with moderate acinar cell loss, inflammatory cell infiltration, and stromal fibrosis, resulting in a pancreatitis score of 6.2±0.8 (Fig. 3A, B). The inflammatory reaction in mutant mice fed the HFCD was similar to HFCD-fed wildtype mice (pancreatitis score of 6.2±0.8 vs. 4.4±1.7). More detailed analyses demonstrated that infiltrating inflammatory cells stained positive for CD3 and F4/80 (Fig. 4), indicating a mixed T-cell and macrophage infiltration into the pancreas of HFCD-fed mutant animals. Only very few B220-positive B-cells were detected (Fig. 4).

Almost no inflammatory cell infiltrates were seen at 14 weeks in mutant mice fed the control diet.

Next, we measured the levels of several cytokines in the pancreas of wildtype and mutant mice fed the CD or HFCD for 3 months. The HFCD significantly increased the levels of several cytokines and chemokines, e.g. eotaxin, G-CSF, M-CSF, LIF, LIX, MCP-1, TNF-α, IL-3, IL-6, and IL-15 in mutant mice compared to mutant animals fed the CD (Fig. 5). No significant differences at 14 weeks of feeding were found in IL-1α and IL-1β (not shown). Interestingly, several cytokines, e.g. eotaxin, G-CSF, MCP-1, IL-6, were elevated in CD-fed mutant animals compared to CD-fed wildtype animals, while the HFCD had no significant effect on several cytokine levels in the pancreas of wildtype mice (Fig. 5).

We also examined the impact of a HFCD on pancreatic stellate cell activation. Immunofluorescence revealed more robust staining for alpha smooth muscle actin (α-SMA), indicating activated pancreatic stellate cells, in mice fed the HFCD (Fig. 6). This was accompanied by an increased deposition of the extracellular matrix protein fibronectin (Fig. 6).

These studies demonstrate that a diet high in fats and calories leads to obesity, metabolic disturbances, and pancreatic inflammation in wildtype and mutant mice.

A diet high in fats and calories accelerates early PanIN development in conditional $Kras^{G12D}$ mice

Next, we sought to determine whether the high fat, high calorie diet accelerates early pancreatic neoplasia. Histological evaluation of pancreatic tissue sections revealed that after 14 weeks mutant mice fed the control diet had mostly normal pancreatic duct morphologies (88.7±2.8%) with scattered mPanIN-1a lesions (10.6±2.8%) and very few mPanIN-1b lesions (0.6±0.3%) (Fig. 7A, B). Mutant mice fed the HFCD displayed significantly less normal pancreatic ducts (45.0±1.9%), more mPanIN-1a (43.6±2.3%), mPanIN-1b (7.2±1.3%), mPanIN-2 (2.4±1.1%), and few mPanIN-3 lesions (1.8±0.8%). During the short period of 14 weeks no invasive pancreatic cancers were seen. Importantly, no pancreatic duct pathologies were seen in wild type mice fed either the control diet or the HFCD.

Discussion

There is great interest in deciphering the mechanisms, by which diet-induced obesity leads to increased risk of developing cancer. Although an association between obesity and cancer is well described, the detailed operative mechanisms are not clearly understood. The purpose of the present study was to develop a model of diet-induced obesity and pancreatic cancer development in a state-of-the-art mouse model, which resembles several important clinical features of human obesity, e.g. weight gain and metabolic disturbances. In that context, oncogenic Kras-driven genetically engineered mouse models of pancreatic cancer have been shown to closely mimic the human responses to therapies and have great potential for biomarker discovery and mechanistic studies (33).

As mentioned before, several earlier studies also indicated that high fat diets enhanced pancreatic carcinogenesis and tumor promotion but did not provide a satisfactory animal model for further mechanistic studies. In particular, mice with a pancreas-specific activation of oncogenic Kras fed a high fat diet showed significantly accelerated PanIN development (26); however, in that study animals on the high fat diet did not gain more weight than control animals and remained insulin sensitive, experienced pancreatic exocrine insufficiency with substantial changes in energy metabolism, which together led to an improved glucose tolerance (26). In stark contrast to that report our results presented here

demonstrate that conditional KrasG12D mice fed a diet high in fats and calories 1) gained significantly more weight, 2) experienced metabolic abnormalities with elevated circulating levels of insulin and IGF-1, 3) did not develop pancreatic exocrine insufficiency, 4) showed marked pancreatic tissue inflammation and acceleration of mPanIN development. Clearly, there are substantial differences between the animal models used in the report of Khasawneh et. al. and the study presented here. It is noteworthy that Khasawneh et. al. used the p48 promoter to drive pancreas-specific expression of oncogenic Kras in mice on a mixed C57BL/6;129 background, while we used mice on a re-derived, pure C57BL/6 background, in which pancreas-specific oncogenic Kras is driven by the Pdx-1 promoter. Different background strains and promoter constructs may account for the observed differences. This is highlighted by a report emphasizing the importance of strain background on the development of diet-induced obesity, inflammation, and PanINs in genetically engineered mouse models of pancreatic cancer (25).

Our HFCD clearly induced an inflammatory reaction in the pancreas with infiltration of mainly macrophages and T-cells, which was seen in wild type as well as mutant mice. This is consistent with other elegant studies, which show prominent infiltration of immune cells with suppressive properties, e.g. tumor-associated macrophages, myeloid-derived suppressor cells, and regulatory T cells, during early pancreatic cancer development in genetically engineered mouse models (34,35). Our analysis of cytokine levels in the pancreas demonstrated a significant elevation of several cytokines and chemokines in the pancreas of mutant animals fed the HFCD. Several colony stimulating factors and chemokines were significantly elevated while other major pro-inflammatory cytokines, e.g. IL-1, were not changed after 14 weeks of feeding the HFCD. The importance of colony stimulating factors was highlighted in a recent report demonstrating that tumor-derived GM-CSF was necessary and sufficient for recruiting immune-suppressive leukocytes into the pancreas and driving tumor development (36). We also found only a slight elevation of TNF-α in the pancreas of mutant mice fed the HFCD for 14 weeks. These data indicate an early robust stimulation of hematopoietic cell lineages and recruitment of inflammatory cells into the pancreas elicited by the HFCD. It is conceivable that at later time points other pro-inflammatory cytokines, e.g. IL-1, TNF-α, produced by the infiltrated immune cells will be highly elevated. Other cytokines, e.g. IL-15, which are important for the stimulation and activation of the immune system, were elevated, indicating a complex immune response in the pancreas of mutant mice fed the HFCD. Interestingly, despite a similar histological picture of pancreatic inflammation in both wildtype and mutant mice fed the HFCD (resulting in a similar pancreatitis index), only mice with the oncogenic Kras mutation showed a marked elevation of several cytokines and chemokines. This indicates a possible re-enforcing crosstalk between the KrasG12D mutation and immune cells in this model.

In our study, only the mutant mice developed mPanIN lesions, indicating that the inflammation alone is not sufficient to initiate pancreatic neoplasia in wildtype C57BL/6 mice. However, compared to control diet-fed animals, the progression of mPanIN lesions in HFCD-fed mutant mice was significantly accelerated in the presence of an inflammatory tissue micro-environment, suggesting that inflammation can act as a tumor promoting factor in KrasG12D-initiated cells. There is a thought that high-fat diet-induced tumor promotion is at least in part mediated by direct effects of diet-induced hyperlipidemia on initiated cells. Our finding that the HFCD did not lead to elevated serum cholesterol and triglycerides levels argues against a direct effect of diet-induced hyperlipidemia on PanIN progression in this model.

The mechanisms proposed to link obesity to increased cancer risk include the development of insulin resistance leading to compensatory high circulating levels of insulin and insulin like growth factor-1 (IGF-1) and inflammation (12,37). High fat, high calorie diet-induced

obesity (with ensuing insulin resistance) is recognized to lead to a chronic, systemic, low-grade inflammatory state with elevations in reactive oxygen species, circulating growth factors, e.g. insulin, IGF-1, pro-inflammatory cytokines, e.g. interleukins and leptin, and eicosanoids (12). This inflammatory milieu may be conducive to tumor promotion and is thought to be the major mechanism, by which chronic pancreatitis leads to PaCa (38,39). Furthermore, a few acute episodes of pancreatitis can also significantly accelerate PanIN development in genetically engineered mouse models of pancreatic cancer (40). Despite the potential clinical importance, studies investigating in detail the mechanisms of diet-induced PaCa in a relevant animal model characterized by obesity and insulin resistance, thereby mimicking the human condition, have been lacking. Our model and presented results are the first step to unravel the underlying mechanisms.

Taken together, our observations strongly suggest that a diet high in fats and calories, which leads to weight gain and metabolic disturbances, can induce pancreatic inflammation and promote pancreatic neoplasia in the presence of an oncogenic Kras mutation. This model, which recapitulates several important clinical features of human obesity with accompanying weight gain and metabolic disturbances, seems ideal to precisely study the kinetics of several pathophysiological processes during diet-induced pancreatic cancer development and investigate the impact of pharmacological interventions on this process. Exact insights of diet-induced obesity and cancer growth are of utmost importance for developing preventive and therapeutic interventions and for formulating dietary recommendations.

Acknowledgments

Financial Support: National Institute of Health (P01 CA163200, P01 AT003960, R01 CA122042), Department of Veterans Affairs, and Hirshberg Foundation for Pancreatic Cancer Research

References

1. Siegel R, Naishadham D, Jemal A. Cancer statistics 2013. CA Cancer J Clin. 2013; 63:11–30. [PubMed: 23335087]
2. Hruban RH, Goggins M, Parsons J, Kern SE. Progression model for pancreatic cancer. Clin Cancer Res. 2000; 6:2969–2972. [PubMed: 10955772]
3. Maitra A, Fukushima N, Takaori K, Hruban RH. Precursors to invasive pancreatic cancer. Adv Anat Pathol. 2005; 12:81–91. [PubMed: 15731576]
4. Kanda M, Matthaei H, Wu J, Hong SM, Yu J, Borges M, et al. Presence of somatic mutations in most early-stage pancreatic intraepithelial neoplasia. Gastroenterology. 2012; 142:730–733. [PubMed: 22226782]
5. Deramaudt T, Rustgi AK. Mutant KRAS in the initiation of pancreatic cancer. Biochim Biophys Acta. 2005; 1756:97–101. [PubMed: 16169155]
6. Hingorani SR, Petricoin EF, Maitra A, Rajapakse V, King C, Jacobetz MA, et al. Preinvasive and invasive ductal pancreatic cancer and its early detection in the mouse. Cancer Cell. 2003; 4:437–450. [PubMed: 14706336]
7. Aguirre AJ, Bardeesy N, Sinha M, Lopez L, Tuveson DA, Horner J, et al. Activated Kras and Ink4a/Arf deficiency cooperate to produce metastatic pancreatic ductal adenocarcinoma. Genes Dev. 2003; 17:3112–3126. [PubMed: 14681207]
8. Hingorani SR, Wang L, Multani AS, Combs C, Deramaudt TB, Hruban RH, et al. Trp53R172H and KrasG12D cooperate to promote chromosomal instability and widely metastatic pancreatic ductal adenocarcinoma in mice. Cancer Cell. 2005; 7:469–483. [PubMed: 15894267]
9. Collins MA, Brisset JC, Zhang Y, Bednar F, Pierre J, Heist KA, et al. Metastatic pancreatic cancer is dependent on oncogenic kras in mice. PLoS One. 2012; 7:e49707. [PubMed: 23226501]
10. Guerra C, Schuhmacher AJ, Canamero M, Grippo PJ, Verdaguer L, Perez-Gallego L, et al. Chronic pancreatitis is essential for induction of pancreatic ductal adenocarcinoma by K-Ras oncogenes in adult mice. Cancer Cell. 2007; 11:291–302. [PubMed: 17349585]

11. Aune D, Greenwood DC, Chan DS, Vieira R, Vieira AR, Navarro Rosenblatt DA, et al. Body mass index, abdominal fatness and pancreatic cancer risk: a systematic review and non-linear dose-response meta-analysis of prospective studies. Ann Oncol. 2012; 23:843–852. [PubMed: 21890910]
12. Bao B, Wang Z, Li Y, Kong D, Ali S, Banerjee S, et al. The complexities of obesity and diabetes with the development and progression of pancreatic cancer. Biochim Biophys Acta. 2011; 1815:135–146. [PubMed: 21129444]
13. Bracci PM. Obesity and pancreatic cancer: overview of epidemiologic evidence and biologic mechanisms. Mol Carcinog. 2012; 51:53–63. [PubMed: 22162231]
14. Lowenfels AB, Maisonneuve P. Risk factors for pancreatic cancer. J Cell Biochem. 2005; 95:649–656. [PubMed: 15849724]
15. Nitsche C, Simon P, Weiss FU, Fluhr G, Weber E, Gartner S, et al. Environmental risk factors for chronic pancreatitis and pancreatic cancer. Dig Dis. 2011; 29:235–242. [PubMed: 21734390]
16. Arslan AA, Helzlsouer KJ, Kooperberg C, Shu XO, Steplowski E, Bueno-de-Mesquita HB, et al. Anthropometric measures, body mass index, and pancreatic cancer: a pooled analysis from the Pancreatic Cancer Cohort Consortium (PanScan). Arch Intern Med. 2010; 170:791–802. [PubMed: 20458087]
17. Hori M, Kitahashi T, Imai T, Ishigamori R, Takasu S, Mutoh M, et al. Enhancement of carcinogenesis and fatty infiltration in the pancreas in N-nitrosobis(2-oxopropyl)amine-treated hamsters by high-fat diet. Pancreas. 2011; 40:1234–1240. [PubMed: 21989024]
18. Sanchez GV, Weinstein SJ, Stolzenberg-Solomon RZ. Is dietary fat, vitamin D, or folate associated with pancreatic cancer? Mol Carcinog. 2012; 51:119–127. [PubMed: 22162236]
19. Xue L, Yang K, Newmark H, Leung D, Lipkin M. Epithelial cell hyperproliferation induced in the exocrine pancreas of mice by a western-style diet. J Natl Cancer Inst. 1996; 88:1586–1590. [PubMed: 8901857]
20. Z'graggen K, Warshaw AL, Werner J, Graeme-Cook F, Jimenez RE, Fernandez-Del CC. Promoting effect of a high-fat/high-protein diet in DMBA-induced ductal pancreatic cancer in rats. Ann Surg. 2001; 233:688–695. [PubMed: 11323507]
21. Zhang J, Go VL. High fat diet, lipid peroxidation, and pancreatic carcinogenesis. Adv Exp Med Biol. 1996; 399:165–172. [PubMed: 8937556]
22. Birt DF, Salmasi S, Pour PM. Enhancement of experimental pancreatic cancer in Syrian golden hamsters by dietary fat. J Natl Cancer Inst. 1981; 67:1327–1332. [PubMed: 6273636]
23. Birt DF, Julius AD, White LT, Pour PM. Enhancement of pancreatic carcinogenesis in hamsters fed a high-fat diet ad libitum and at a controlled calorie intake. Cancer Res. 1989; 49:5848–5851. [PubMed: 2790796]
24. White PB, Ziegler KM, Swartz-Basile DA, Wang SS, Lillemoe KD, Pitt HA, et al. Obesity, but not high-fat diet, promotes murine pancreatic cancer growth. J Gastrointest Surg. 2012; 16:1680–1685. [PubMed: 22688418]
25. Cheon EC, Strouch MJ, Barron MR, Ding Y, Melstrom LG, Krantz SB, et al. Alteration of strain background and a high omega-6 fat diet induces earlier onset of pancreatic neoplasia in EL-Kras transgenic mice. Int J Cancer. 2011; 128:2783–2792. [PubMed: 20725998]
26. Khasawneh J, Schulz MD, Walch A, Rozman J, Hrabe de AM, Klingenspor M, et al. Inflammation and mitochondrial fatty acid beta-oxidation link obesity to early tumor promotion. Proc Natl Acad Sci U S A. 2009; 106:3354–3359. [PubMed: 19208810]
27. Abate-Shen C, Brown PH, Colburn NH, Gerner EW, Green JE, Lipkin M, et al. The untapped potential of genetically engineered mouse models in chemoprevention research: opportunities and challenges. Cancer Prev Res (Phila). 2008; 1:161–166. [PubMed: 19138951]
28. Harris DM, Srihari P, Go VL. Pancreatic cancer prevention and the 2010 Dietary Guidelines for Americans. Pancreas. 2011; 40:641–643. [PubMed: 21673534]
29. Mohammed A, Janakiram NB, Lightfoot S, Gali H, Vibhudutta A, Rao CV. Early detection and prevention of pancreatic cancer: use of genetically engineered mouse models and advanced imaging technologies. Curr Med Chem. 2012; 19:3701–3713. [PubMed: 22680929]

30. Funahashi H, Satake M, Dawson D, Huynh NA, Reber HA, Hines OJ, et al. Delayed progression of pancreatic intraepithelial neoplasia in a conditional Kras(G12D) mouse model by a selective cyclooxygenase-2 inhibitor. Cancer Res. 2007; 67:7068–7071. [PubMed: 17652141]

31. Gier B, Matveyenko AV, Kirakossian D, Dawson D, Dry SM, Butler PC. Chronic GLP-1 receptor activation by exendin-4 induces expansion of pancreatic duct glands in rats and accelerates formation of dysplastic lesions and chronic pancreatitis in the Kras(G12D) mouse model. Diabetes. 2012; 61:1250–1262. [PubMed: 22266668]

32. Hruban RH, Adsay NV, Albores-Saavedra J, Compton C, Garrett ES, Goodman SN, et al. Pancreatic intraepithelial neoplasia: a new nomenclature and classification system for pancreatic duct lesions. Am J Surg Pathol. 2001; 25:579–586. [PubMed: 11342768]

33. Singh M, Murriel CL, Johnson L. Genetically engineered mouse models: closing the gap between preclinical data and trial outcomes. Cancer Res. 2012; 72:2695–2700. [PubMed: 22593194]

34. Clark CE, Beatty GL, Vonderheide RH. Immunosurveillance of pancreatic adenocarcinoma: Insights from genetically engineered mouse models of cancer. Cancer Lett. 2009; 279:1–7. [PubMed: 19013709]

35. Clark CE, Hingorani SR, Mick R, Combs C, Tuveson DA, Vonderheide RH. Dynamics of the immune reaction to pancreatic cancer from inception to invasion. Cancer Res. 2007; 67:9518–9527. [PubMed: 17909062]

36. Bayne LJ, Beatty GL, Jhala N, Clark CE, Rhim AD, Stanger BZ, et al. Tumor-derived granulocyte-macrophage colony-stimulating factor regulates myeloid inflammation and T-cell immunity in pancreatic cancer. Cancer Cell. 2012; 21:822–835. [PubMed: 22698406]

37. Giovannucci E, Michaud D. The role of obesity and related metabolic disturbances in cancers of the colon, prostate, and pancreas. Gastroenterology. 2007; 132:2208–2225. [PubMed: 17498513]

38. Jura N, Archer H, Bar-Sagi D. Chronic pancreatitis, pancreatic adenocarcinoma and the black box in-between. Cell Res. 2005; 15:72–77. [PubMed: 15686632]

39. Whitcomb DC. Inflammation and Cancer V. Chronic pancreatitis and pancreatic cancer. Am J Physiol Gastrointest Liver Physiol. 2004; 287:G315–G319. [PubMed: 15246966]

40. Carriere C, Young AL, Gunn JR, Longnecker DS, Korc M. Acute pancreatitis markedly accelerates pancreatic cancer progression in mice expressing oncogenic Kras. Biochem Biophys Res Commun. 2009; 382:561–565. [PubMed: 19292977]

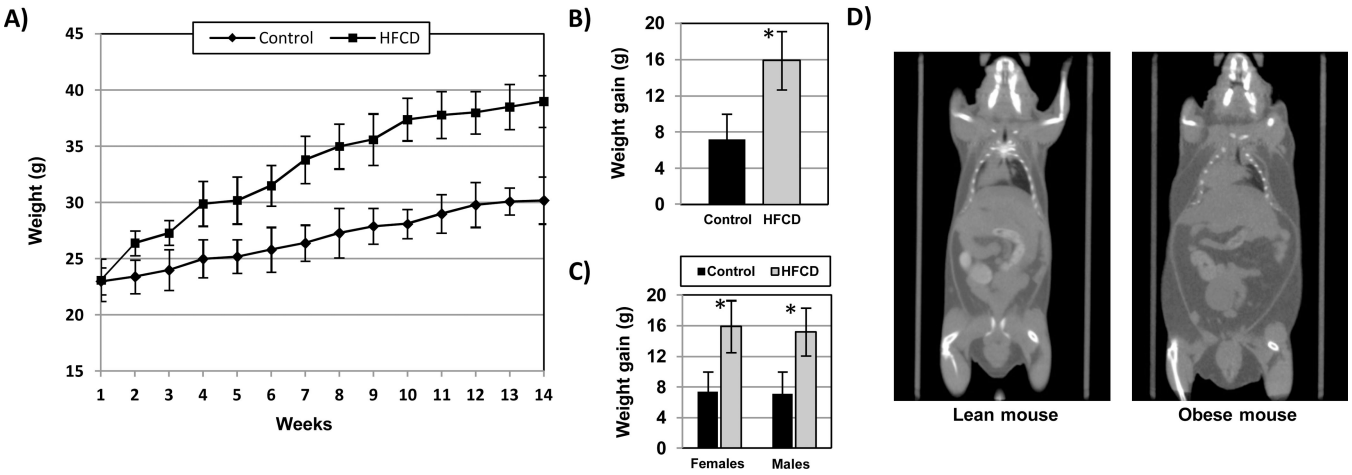

Figure 1.

A) Weekly measurements of weight (in grams) of mice fed the control or high fat, high calorie diet (HFCD). Data are depicted as average ± SD. **B)** Weight gain (in grams) after 14 weeks of mice fed the control diet or HFCD. Data are depicted as average ± SD. *; $p<0.05$ vs. control. **C)** Weight gain (in grams) after 14 weeks of female and male mice fed the control diet or HFCD. Data are depicted as average ± SD. *; $p<0.05$ vs. control. **D)** Representative micro-CT images of a lean mouse (left panel) and obese mouse (right panel).

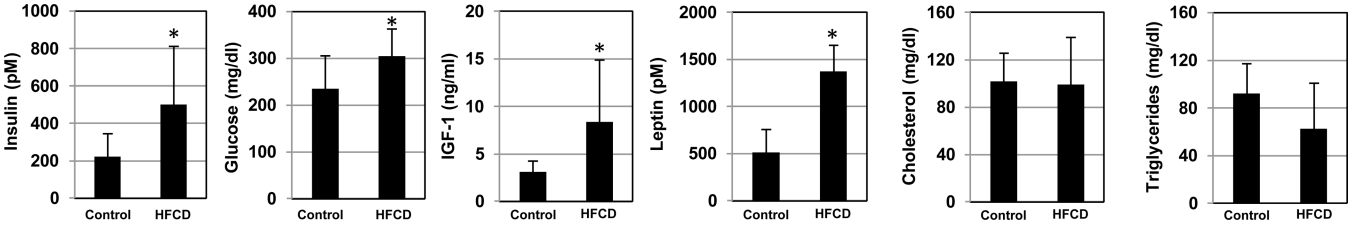

Figure 2.

Serum levels of insulin, glucose, insulin-like growth factor-1 (IGF-1), leptin, cholesterol, and triglycerides at 14 weeks of mice fed the control diet or HFCD. Data are depicted as average ± SD. *; $p<0.05$ vs. control.

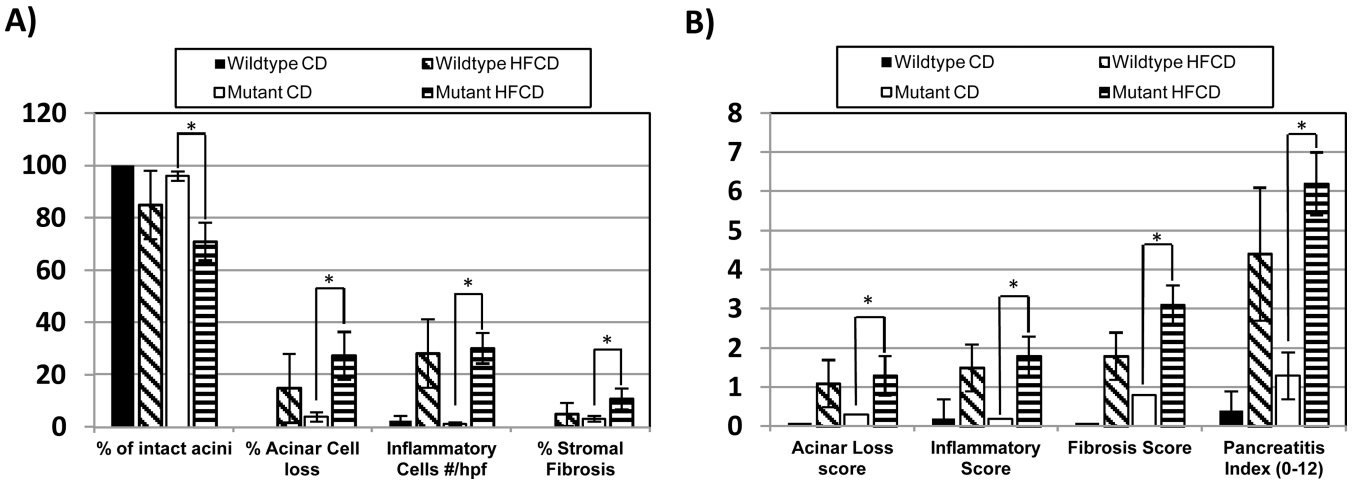

Figure 3.

Semi-quantitative analyses of inflammatory parameters in the pancreas of mice fed the control diet or HFCD. **A)** Percentage (%) of intact acini, percentage (%) of acinar cell loss, number of inflammatory cells per high power field (hpf), and percentage (%) of stromal fibrosis are analyzed separately for wildtype and mutant mice fed the control diet or HFCD. *; $p<0.05$. **B)** Acinar loss score, inflammatory score, fibrosis score, and pancreatitis index in wildtype and mutant mice fed the control diet or HFCD. *; $p<0.05$.

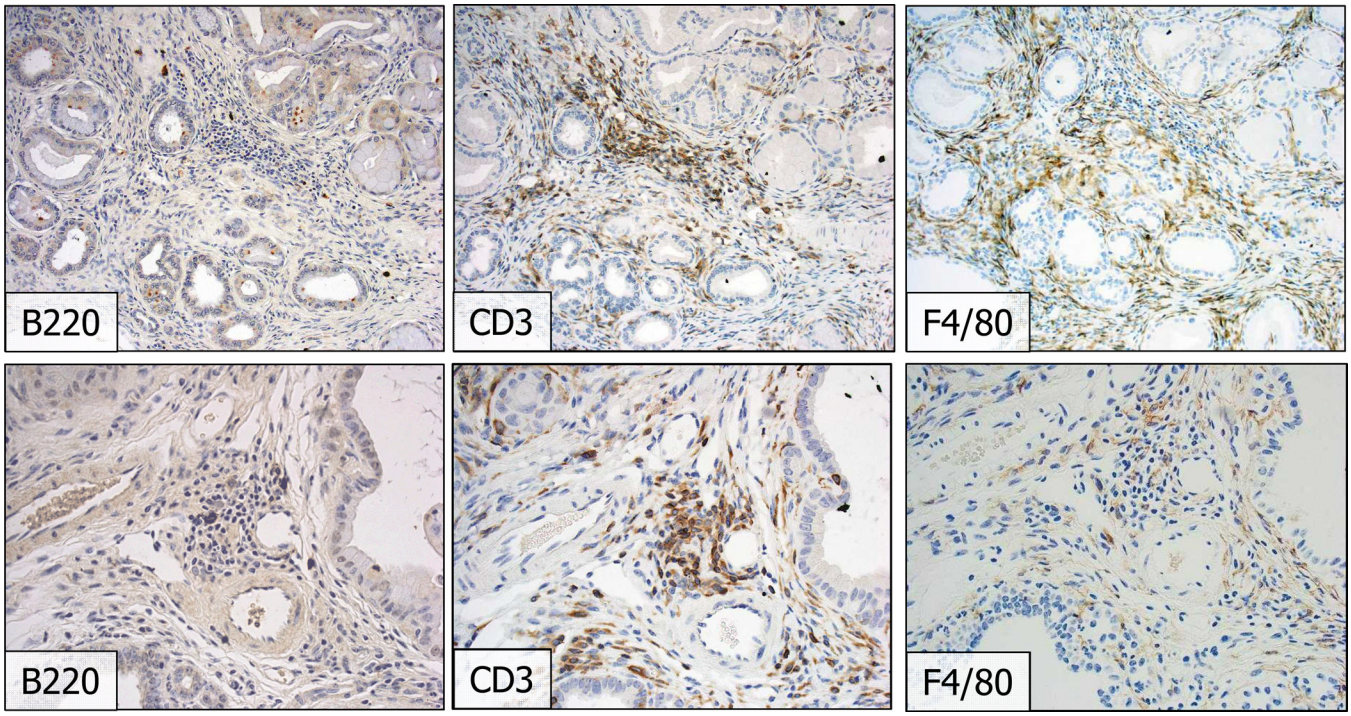

Figure 4.

Immunohistochemistry of infiltrating immune cells into the pancreas of conditional KrasG12D mice fed the HFCD. Tissue sections were stained with antibodies against B220 (B-cell marker), CD-3 (T-cell marker), and F4/80 (macrophage marker). Upper row is 200× magnification and lower row is higher 400× magnification.

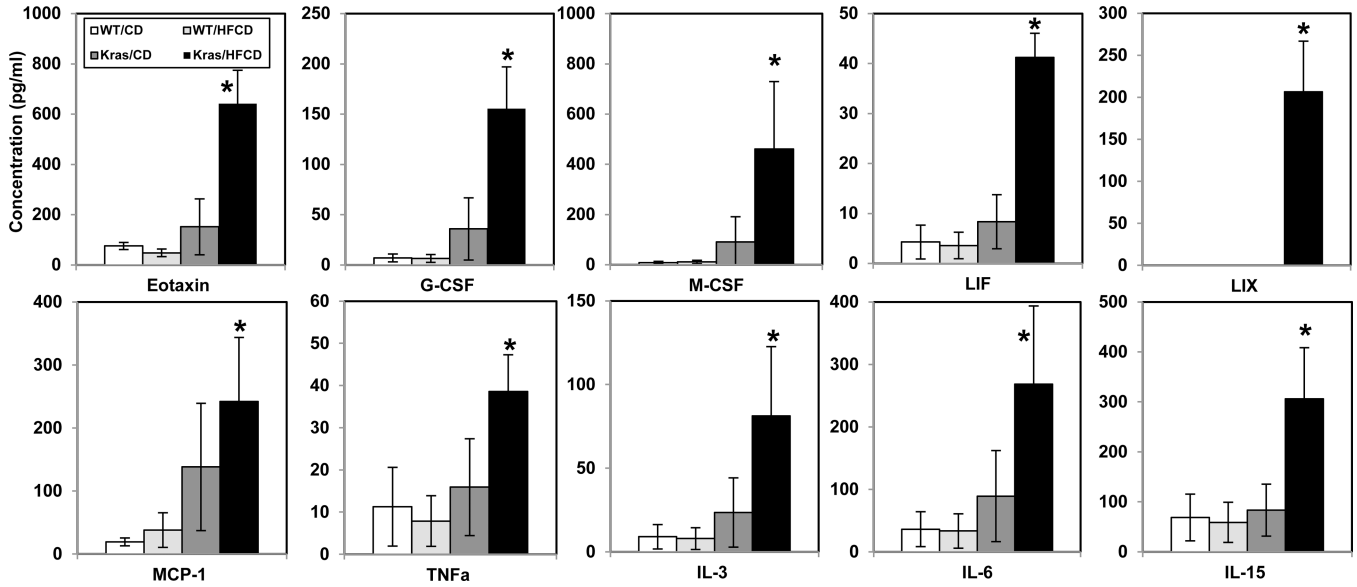

Figure 5.

Cytokine and chemokine levels were measured in the pancreas of wildtype (WT) and conditional KrasG12D (Kras) mice fed either the control diet (CD) or high fat, high calorie diet (HFCD). Data are depicted as average ± SD. *; $p<0.05$ vs. CD.

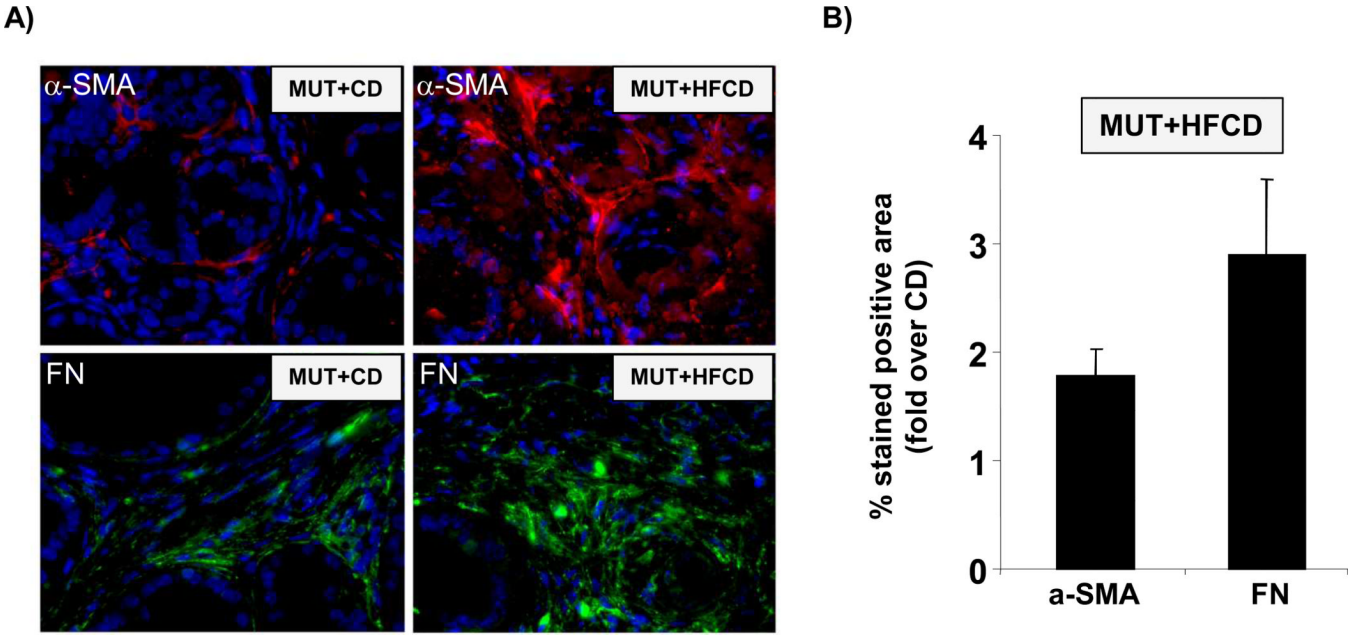

Figure 6.

Immunofluorescence staining of α-smooth muscle actin (a-SMA, marker of active pancreatic stellate cells; red staining) and fibronectin (FN, green staining) in conditional KrasG12D mice (MUT) fed the control diet (CD) or a high-fat, high-calorie (HFCD) diet for 3 months. Blue staining represents DAPI-positive nuclei. Magnification, ×400. B) Graph shows quantification of and α-SMA and FN staining in pancreatic tissue sections. Data are depicted as average ± SD.

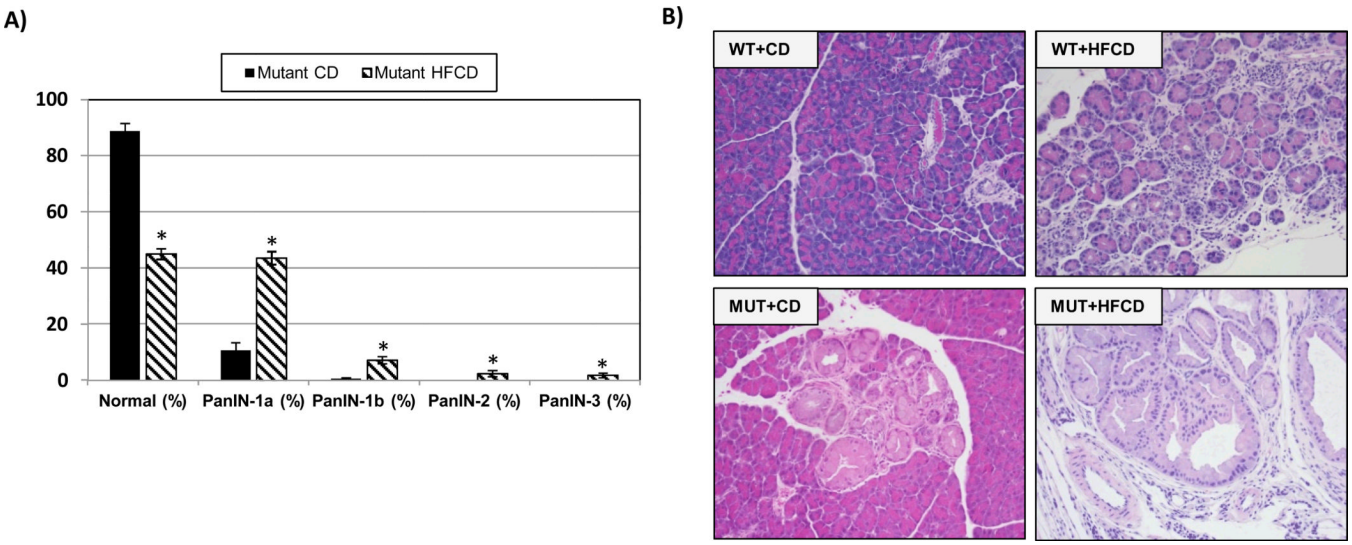

Figure 7.

A) Distribution (in %) of normal pancreatic ducts and mPanIN-1a, mPanIN-1b, mPanIN-2 and mPanIN-3 lesions in the pancreas of mutant mice fed the control diet or HFCD. *; $p<0.05$ vs. mutant CD. **B)** Representative H.E. staining of pancreatic tissue sections at 14 weeks: Wildtype mice fed the control diet; wildtype mice fed the HFCD; mutant mice fed the control diet; mutant mice fed the HFCD.

Table 1

Composition of control and experimental diet

	AIN-76A			HFCD		
	kcal/gm	**grams/kg**	**kcal/kg**	**kcal/gm**	**grams/kg**	**kcal/kg**
Casein	3.58	200	716	3.58	200	716
Sucrose	4	380.8	1,523.2	4	380.8	1,523.2
Cornstarch	3.6	269.2	969.12	3.6	119.2	429.12
Cellulose	0	50	0	0	50	0
Corn Oil	9	50	450	9	200	1,800
DL-Methionine	4	3	12	4	3	12
Salt Mix	0.47	35	16.45	0.47	35	16.45
Vitamin Mix	3.92	10	39.2	3.92	10	39.2
Choline Bitartrate	0	2	0	0	2	0
		1000	**3,725.97**		**1000**	**4,535.97**